Propagation of classical waves in nonperiodic media: Scaling properties of an optical Cantor filter

A. V. Lavrinenko,[1] S. V. Zhukovsky,[1,2] K. S. Sandomirski,[2] and S. V. Gaponenko[2,*]
[1]*Physics Department, Belarusian State University, Minsk 220080, Belarus*
[2]*Institute of Molecular and Atomic Physics, National Academy of Sciences of Belarus, Minsk 220072, Belarus*
(Received 5 August 2001; published 7 March 2002)

Wave propagation through a subclass of deterministic nonperiodic media, namely, fractal Cantor multilayer structures are investigated theoretically as well as experimentally. Transmission spectra of Cantor structures are found to have two distinctive properties (*scalability* and *sequential splitting*) closely related to the geometrical peculiarities of the multilayers. A systematic correlation between structural self-similarity and spectral regularities of Cantor multilayers is established.

DOI: 10.1103/PhysRevE.65.036621 PACS number(s): 42.70.Qs, 68.65.Ac, 78.20.Bh, 61.43.Hv

I. INTRODUCTION

As regards the problem of wave propagation in complex media, the last decade was most prominent in establishing the properties of both perfectly periodic and absolutely random media. On one hand, it was shown that internal periodicity underlying the design of photonic crystals gives the possibility to obtain complete and absolute photonic band gap for optical radiation [1–3], thus providing vast contribution to optoelectronic applications, and on the other hand, the idea of light localization in random media has been intensively explored. This idea was greatly inspired by the first theories and experiments [4–6].

Nonperiodic but deterministic media constitute a separate field of research. One can expect their properties can unite forbidden gaps in transmission spectra with strong resonances, which can localize light very effectively. In some manner the properties of such media remind of those of periodic ones with embedded defects, while possessing some properties of random media as well. This idea was first discovered during extensive research of wave phenomena in fractal lattices (namely, critical phenomena, spin, and percolation studies) that started quite a while ago (see, e.g., Refs. [7–9]) and remains worth close attention for modern science.

Recent investigations of the physical properties of various groups of these deterministic media, namely, substitutional (Fibonacci, Thue-Morse, Rudin-Shapiro, and double-period) sequences [10–20,22,23] or model fractal structures (Cantor sets or Koch fractals) [21–25] have revealed that such structures exhibit certain distinctive features compared to traditional (that is, periodic and random) media. These features have become an object of great interest for scientists.

In the present paper, we focus on Cantor sets of dielectric isotropic layers. The structures of this type are investigated theoretically as well as experimentally. A one-dimensional (1D) problem of classical wave propagation through a medium with stepwise-changing parameter (dielectric constant for electromagnetic and material density for acoustic waves), isomorphic to a one-dimensional problem of a quantum mechanical particle in a stepwise potential, is numerically solved for Cantor structures.

This paper is organized as follows. First, in Sec. II, a reader is introduced to the theoretical background, such as details on Cantor multilayers. There we also describe a simple but effective technique used for computational procedures. The distinctive properties found as a result of the modeling and the discussion thereof is what follows in Secs. III and IV. Finally, in Sec. V, we present experimental results and provide comparison with theoretical ones. Section VI summarizes the paper.

It is also worth noting here that fractal structures, while being relatively new to physical research if compared to continuous media and thus investigated not as thoroughly as desired, represent an object of particular interest for modern science. Fractal objects are found everywhere, from geography to nonlinear dynamics [26]. This way, the paper also contributes to the research of fractal structures, in general, Cantor stacks being only a model.

II. THEORETICAL BACKGROUND

Prior to proceeding with the description of calculation procedures we used, it is essential to touch briefly upon some underlying concepts. At first, let us note that deterministic nonperiodic media lack a neat and generally accepted classification. The attempts have been made to classify such media taking into account their singularity spectrum [18], but it has not been thoroughly worked on yet. However, most authors agree on separating multilayered media accordingly to the construction algorithm, thus distinguishing two major groups, namely, the *substitutional lattices* (Fibonacci, Thue-Morse, Rudin-Shapiro, etc.), generated via repeated substitution procedure, and the *model fractal multilayers* (Cantor and Koch fractals) that are constructed in a way similar to fractal sets [26]. It is also interesting to remark that *quasiperiodicity*, in its mathematical definition (quasiperiodic structures are those composed of two or more incommensurate periods [18,19]), stands somewhat apart from both of the groups. For instance, Fibonacci multilayer stacks *are* quasiperiodic, while Rudin-Shapiro stacks *are not*.

A. Cantor-like multilayers

As was mentioned above, Cantor-like structures are fractal nonperiodic multilayers generated in a way similar to the

*Email address: gaponen@imaph.bas-net.by

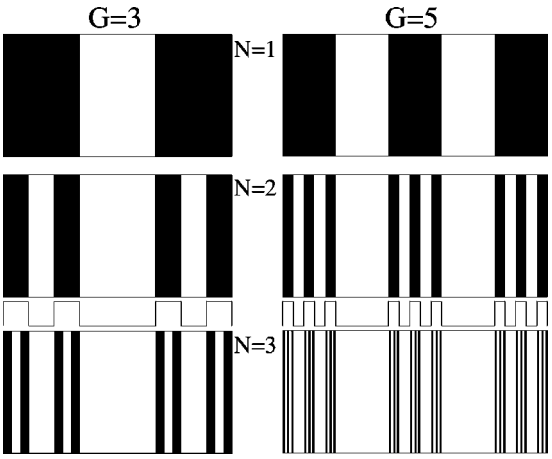

FIG. 1. Cantor multilayer structures for smaller numbers of G and N. Dark and light areas indicate high- and low-index materials, respectively.

Cantor set construction [26]. Any Cantor multilayer is characterized by two fundamental parameters, the *generator* $G=3,5,7,\ldots$ and the *generation number* $N=1,2,3,\ldots$. Take a *seed* to be a bulk of a dielectric (labeled A). Then replace the certain parts of the seed (determined by the value of G) with another dielectric material (labeled B). Then repeat the same procedure over all the remaining inclusions of the initial material, as if they were seeds. When these steps are recurred N times, the resulting structure will be a Cantor multilayer characterized by a pair of numbers (G,N), or, as it will be called hereafter, *a* (G,N) *structure*. Sample structures are shown in Fig. 1, and the stack construction methods can be easily understood therefrom. As we see, a (G,N) Cantor multilayer consists of G^N layers. Furthermore, simple scaling relations similar to those found in Ref. [26] allow us to derive an expression for the fractal dimensionality D of a Cantor set underlying a (G,N) structure. It can be attributed to this structure and equals

$$D=\frac{\ln\left(\frac{G+1}{2}\right)}{\ln G}. \tag{1}$$

Finally, note that we have to allow for different velocity of light in various media, so whenever the index of refraction $n\neq 1$, the optical thickness of a layer will differ from the geometrical one. For both calculations and measurements, layer thicknesses are chosen to satisfy the condition $n_1d_1=n_2d_2$, the refractive indices of the dielectrics used being equal to n_1 and n_2, and the geometrical thicknesses being equal to d_1 and d_2, respectively. The total geometrical thickness of the stack then is

$$d=\left(\frac{G+1}{2}\right)^N d_1+\left[G^N-\left(\frac{G+1}{2}\right)^N\right]d_2. \tag{2}$$

B. On the calculation of transmission spectra for multilayers

Before we start up with the theoretical procedure used in our calculations let us outline commonly used methods. As most of structures under consideration are stratified media with different sequences of layers, every method developed for 1D inhomogeneous systems can be applied for this problem. There are several fundamental monographs [27–31] where one can find all necessary information about standard methods.

We restrict ourselves to discrete inhomogeneous systems, when inhomogeneity only occurs in a finite set of points, namely, at borders between layers. The layers themselves are homogeneous, isotropic, and infinite in two transverse directions. In such cases an analogy between electrodynamics and quantum mechanics (or, from a mathematical standpoint, between Helmholtz and Schrödinger equations) appears to be rather fruitful. The role of potential energy is now taken by a function that solely depends on dielectric permittivity of media. In multilayer structures the latter has a stepwise profile with a limited number of discontinuity points, so it can be handled properly by calculating the jumps of certain field components at the layer interfaces. Thus nearly all existing methods are based on matrix calculus (see Refs. [27–31]).

In spite of presence of fairly rigorous and straightforward matrix methods, we would like to introduce here a simpler and therefore faster method of fields restoration, implemented deliberately for application in problems of 1D propagation in nonperiodic stacks of isotropic layers. As will be seen later, we only use ''one half'' of usual calculations needed for deriving a transfer matrix. And although we had to sacrifice the power of matrix algebra, we nevertheless tailored another technique, which helped us to reduce the computer time required for the calculations by ten times compared to procedure involving 4×4 matrices and by a couple of times compared to 2×2 matrices, as regards transmission spectra of Cantor multilayers. Thus, it enables us to investigate systems involving very large numbers of layers, which is rather useful in many respects.

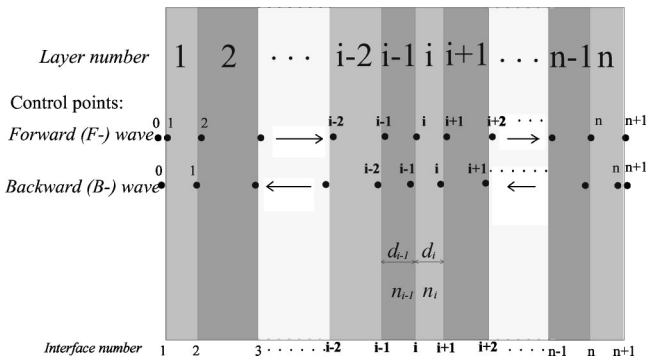

FIG. 2. A typical multilayer structure with the set of control points and numbering conventions used in the calculation procedure.

C. The calculation procedure

Consider a multilayer consisting of M layers, the index of refraction, and thickness of the jth layer in the stack defined as n_j and d_j, respectively (see Fig. 2). A plane wave

$$\mathbf{E}_0(\mathbf{r},t)=\mathbf{E}_0\exp(i\omega t-i\mathbf{k}\cdot\mathbf{r}), \tag{3}$$

characterized by vector amplitude $\mathbf{E}_0$, frequency ω, and wave vector $\mathbf{k}$ is impinging on the stack normally to its surface. (For clarity, we will consider the normal incidence case first, then we will provide a generalization for arbitrary angle of incidence). Multiple reflections redistribute electromagnetic fields in the stack. Due to the linearity of the media a field pattern in all points is a result of an interference between forward- and back-going waves, labeled further by F and B. At any given point

$$\mathbf{E}(\mathbf{r},t)=\mathbf{E}_F\exp(i\omega t-i\mathbf{k}\cdot\mathbf{r})+\mathbf{E}_B\exp(i\omega t+i\mathbf{k}\cdot\mathbf{r}). \quad (4)$$

Provided that these two waves are known at some given point of a homogeneous layer, it is easy to restore the field distribution in every point inside the homogeneous layer simply by taking into account phase shifts. An expansion of the procedure to the whole structure leads us to a conclusion that it is enough to know the fields in one point for each of the two waves per layer. These points can be chosen arbitrarily, and a set of such points defined in a stack will be referred to as *control points*. We chose two sets of such points (one for the F waves and another for the B waves) in the immediate vicinity to each of the boundaries from both sides thereof. This system of control points is depicted in Fig. 2.

Reflection $R_{j/(j-1)}$, $R_{(j-1)/j}$ and transmission $T_{j/(j-1)}$, $T_{(j-1)/j}$ coefficients at the layer interfaces are also well known. They are Fresnel's coefficients [28], which are polarization insensitive for normal incidence.

Now consider the propagating waves inside the jth layer. The forward wave $\mathbf{E}_{Fj}$ results, on one hand, from the F wave in $(j-1)$th layer transmitted through the $(j-1)/j$ interface and, on the other hand, from the B wave reflected at $j/(j-1)$ interface (which is the same boundary). So $\mathbf{E}_{Fj}$ is

$$\mathbf{E}_{Fj}=T_{(j-1)/j}t_{F(j-1)}\mathbf{E}_{F(j-1)}+R_{j/(j-1)}t_{Fj}\mathbf{E}_{Bj}. \quad (5)$$

Phase shifts are taken into account by the spatial evolution factors t_{Fj}, which are

$$t_{Fj}=\exp\left(-i\frac{\omega}{c}d_j\right). \quad (6)$$

The similar considerations lead to the B wave field in the corresponding control point inside the jth layer

$$\mathbf{E}_{Bj}=T_{(j+1)/j}t_{B(j+1)}\mathbf{E}_{B(j+1)}+R_{j/(j+1)}t_{Bj}\mathbf{E}_{Fj}. \quad (7)$$

Here the phase factor t_{Bj} differs from t_{Fj} (6) only by the sign of the exponent index.

Equations (5) and (7) allow to calculate the field in any control point of the stack using the field in two neighboring points.

Now assume that the field is known in both control points inside the jth layer. Then the F field that must emerge from the previous layer can easily be derived based on the inversion of Eq. (5). A simple algebra with this equation yields finally,

$$\mathbf{E}_{F(j-1)}=t^{-1}_{F(j-1)}T^{-1}_{(j-1)/j}[\mathbf{E}_{Fj}-R_{j/(j-1)}t_{Fj}\mathbf{E}_{Bj}]. \quad (8)$$

This *restoration formula* is key for all numerical procedure of field calculation. Its "mate" for B wave comes from expression (7) in exactly the same manner as Eq. (8) does from Eq. (5), so the restoration direction can be reversed

$$\mathbf{E}_{B(j+1)}=t^{-1}_{B(j+1)}T^{-1}_{(j+1)/j}[\mathbf{E}_{Bj}-R_{j/(j+1)}t_{Bj}\mathbf{E}_{Fj}]. \quad (9)$$

Keeping in mind that it is necessary to calculate transmission and reflection of the multilayer stack as well as to find out the field distribution inside each layer, suppose that the wave is impinging onto the stack from one side only (the left one in Fig. 2). Then, certainly, the vector $\mathbf{E}_{B(n+1)}=0$. Assigning a temporary arbitrary nonzero value to the vector $\mathbf{E}_{F(n+1)}$, it is possible to find $\mathbf{E}_{Fn}$ via Eq. (8). Then application of Eq. (7) gives the field $\mathbf{E}_{Bn}$. Thus, both fields in the nth layer are obtained. One can see that application of Eqs. (8) and (7) once again yields both waves in the $(n-1)$th layer. Consequent movement from the rightmost layer to the leftmost allows to restore the full picture of relative field distribution in the whole multilayer structure.

The final step consists in scale renormalization. As a result of the whole calculation, we have obtained the value of $\mathbf{E}_{F0}$, which is the incident wave amplitude. If it were equal to one, then reflection and transmission coefficients would simply equal $\mathbf{E}^2_{B0}$ and $\mathbf{E}^2_{F(n+1)}$, respectively. However, it is improbable that this condition is achieved as $\mathbf{E}_{F(n+1)}$ had been chosen arbitrarily. So, a unity is to be manually *assigned* to the incident wave amplitude with rescaling of all other amplitudes, including $\mathbf{E}_{F(n+1)}$, in the same proportion. If we are not interested in the fields inside the layers such scaling procedure results only in two divisions of scalar quantities.

The generalization of the described procedure for an oblique incidence case is rather straightforward. The only thing that has to be done is to replace Fresnel's reflection and transmission coefficients for normal incidence with those for oblique incidence [28]. However, in this case different wave polarizations (TE and TM) yield different coefficients, so it is necessary to write out formulas (5), (7)–(9) separately for each polarization. The phase factor (6) will also change, taking into account the change in the layer thicknesses connected with the inclined propagation in the medium.

III. SCALABILITY OF OPTICAL SPECTRA

At first, let us compare the transmission spectra of Cantor stacks with those of well-studied periodic multilayers. For comparison, it is natural to use stacks with the same number of layers and it is reasonable to choose the model materials with high refractive index contrast $(n_B/n_A=2.3)$ in order to clearly demonstrate all the similarities and differences in spectral properties. Since our stacks are quarter wave, the spectra will be periodic with period equal to $2\omega_0$, where ω_0 is central frequency. Figure 3 shows one period of spectrum for such structures.

As follows from general considerations, both graphs exhibit stop bands (or *band gaps*) and both graphs have the same number of transmission peaks (*resonances*) per period. However, the distribution of peaks is completely different. The overall width of the forbidden gap is larger for the Can-

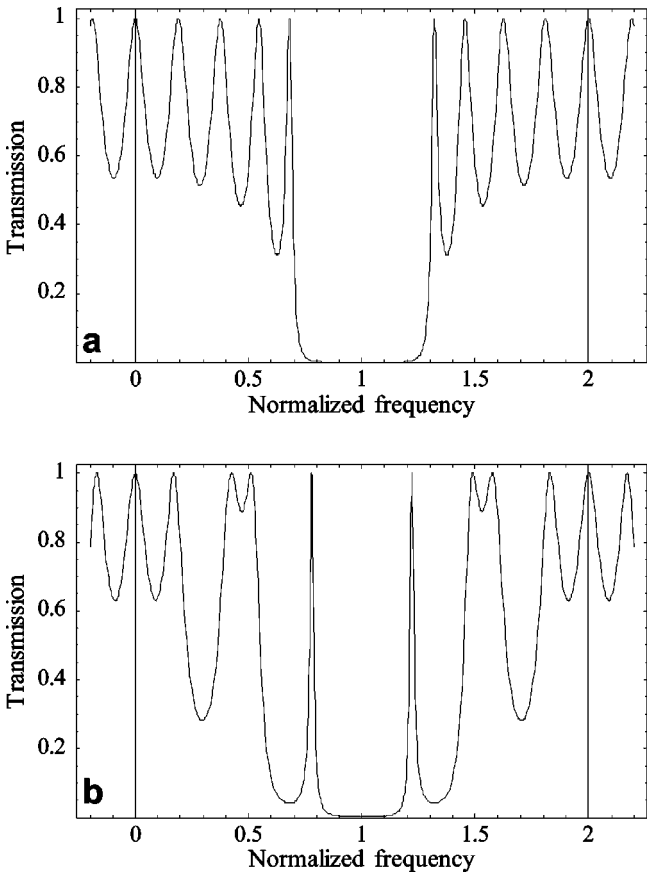

FIG. 3. Transmission spectra for a Cantor multilayer [(a), $G=3$, $N=2$, 9 layers] and a periodic multilayer [(b), 9 layers] in comparison. Note the width of a forbidden gap, the presence of sharp resonance peaks inside the gap, and peak distribution in a Cantor spectrum.

tor structure, but the latter has sharp resonances inside the gap.

These properties have the same underlying physical reasons as those of a Fabry-Pérot dielectric microcavity. We can regard a Cantor structure as a periodic multilayer with a large number of embedded defects. It is known [1] that a defect in a periodic structure results in a *defect state* somewhere in the spectrum, causing one or more transmission peaks to shift into the ''forbidden'' area and other peaks to rearrange. It is also known that such a defect state can be identified by a strong field localization inside the defect at the corresponding frequency.

Based on the analysis of spectra for a large variety of Cantor structures, we have found that the spectra of all Cantor structures exhibit apparent *scalability*. That is, the *whole* spectrum of a (G,N) stack appears as a part of a $(G,N+1)$ stack spectrum. If we magnify the central part of the latter by a factor of G, it will match the former spectrum almost perfectly.

We have found that this property holds for any G, and the factor by which one has to enlarge the central part of the (G,N_1) stack spectrum for matching with that of (G,N_2) stack [termed the *scaling factor* between the (G,N_1) and (G,N_2) spectra] is $G^{N_1-N_2}$. (It is assumed without loss of generality that $N_1>N_2$.) So, this scalability is characteristic to *any* Cantor-like structure. Figures 4 and 5 show this for $G=3$ and $G=5$ structures.

We state that scalability of the spectra results from the self-similarity of the structures. Any (G,N) Cantor structure encompasses the structures of all previous generations (see Fig. 1). Besides, the scaling factor is connected with G and N in exactly the same way. It is natural to expect that this ''structural scalability'' will result in ''spectral scalability.'' However, $(G,N-1)$ structures are contained in a (G,N) structure multiple times (two for $G=3$, three for $G=5$, etc.), while the spectrum is contained only *once*, as can be seen in Figs. 4 and 5. So, the passing wave is insensitive to the number of substructures within the whole stack from the point of view of scalability properties. It *is* sensitive to that number in some other way, which will be described below.

IV. SEQUENTIAL SPLITTING

Note [see Figs. 4(a) and 5(a)] that some resonances in the Cantor stack spectra turn out to be single peaks, while other are multiplets (e.g., doublets). This is a manifestation of another property of Cantor multilayers, which is worth close attention.

We have found a (G,N) stack spectrum has multiplets at the frequencies where a $(G,N-1)$ stack spectrum has single peaks, while new peaks (single or multiplets) in a (G,N) correspond to no peaks in a $(G,N-1)$ and ''appear'' in the forbidden gaps of the latter structure as N is increased. The number of components in the multiplets equals $(G+1)/2$, and, of course, the total number of peaks in one period equals the number of layers, i.e., G^N. As we see in Fig. 6 for $G=3$ and 5, splitting occurs each time we increase the generation. That is why we have termed this property *sequential splitting*.

The reason of such splitting is understood from the point of view of self-similarity of Cantor structures regarded in terms of coupled cavities. As the Cantor algorithm generates a fractal structure, an N_0th generation stack contains all the structures with $N<N_0$ and the same G. For example, a $(G=3,N=4)$ stack contains two inclusions of $(G=3,\ N=3)$ stacks. Then we can make a statement that each single peak in the spectrum of a (3, 4) stack, being a resonant mode introduced by the central ''cavity'' (or layer), splits into a doublet because there are two such cavities in a (4, 4) stack. Two new peaks have to appear in the (4, 4) spectrum, corresponding to the central cavity in this structure, and those peaks must be single, as there is only one such cavity present. It is obvious that the same reasoning applies to any generation, so all single peaks in the spectra of $(3,N)$ structures will split into doublets in the $(3,N+1)$ structures' spectra. Analogous considerations lead to the conclusion that in the case of $G=5$ single peaks will split into triplets and new resonances will appear as doublets, in full accordance with Fig. 6(b). Generalization of this statement results in a formula for the number of components S_{split} in multiplets that have just split and for the number of components S_{new} in newly appearing multiplets, respectively,

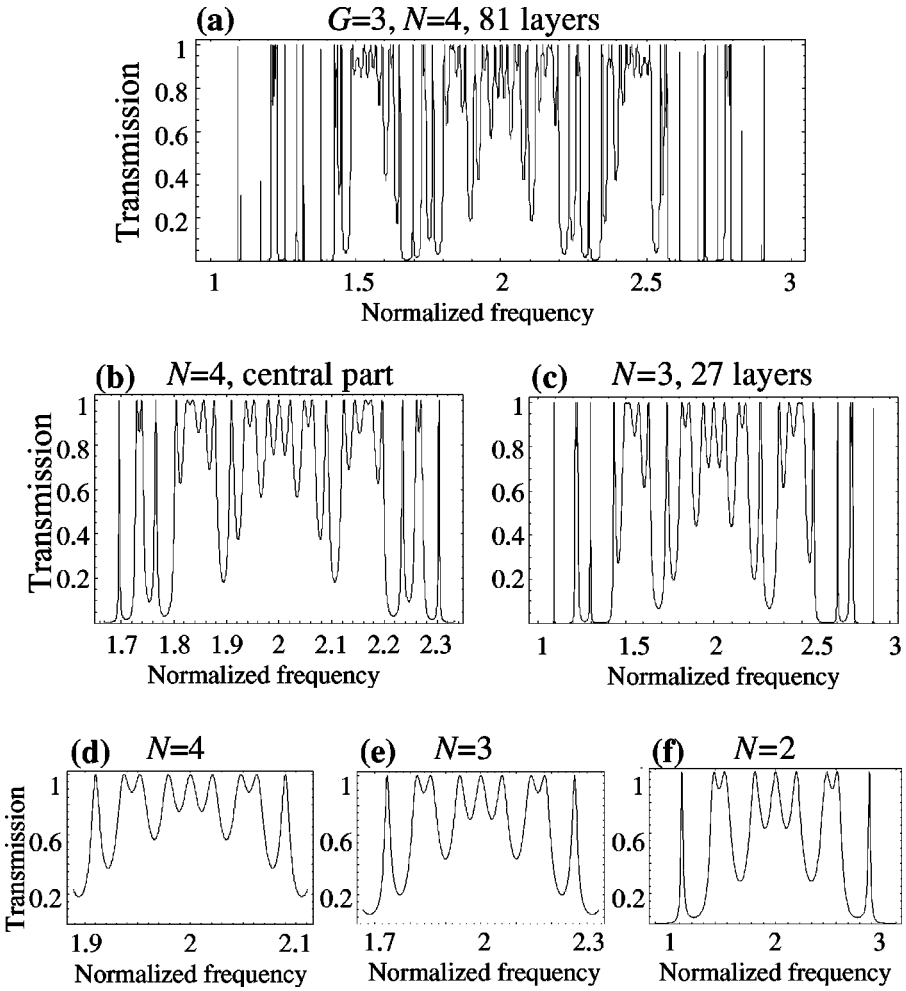

FIG. 4. Scalability of optical spectra for Cantor multilayers ($G=3$): the full period of a (3,4) spectrum (a); the central part of it magnified in the frequency scale by 3 (b) versus the full period of a (3,3) spectrum (c); the central part of (3,4) magnified by $9=3^2$ (d); the central part of (3,3) magnified by 3 (e); the full period of a (3,2) spectrum (f). Compare the looks of (b) and (c), as well as of (d), (e), and (f).

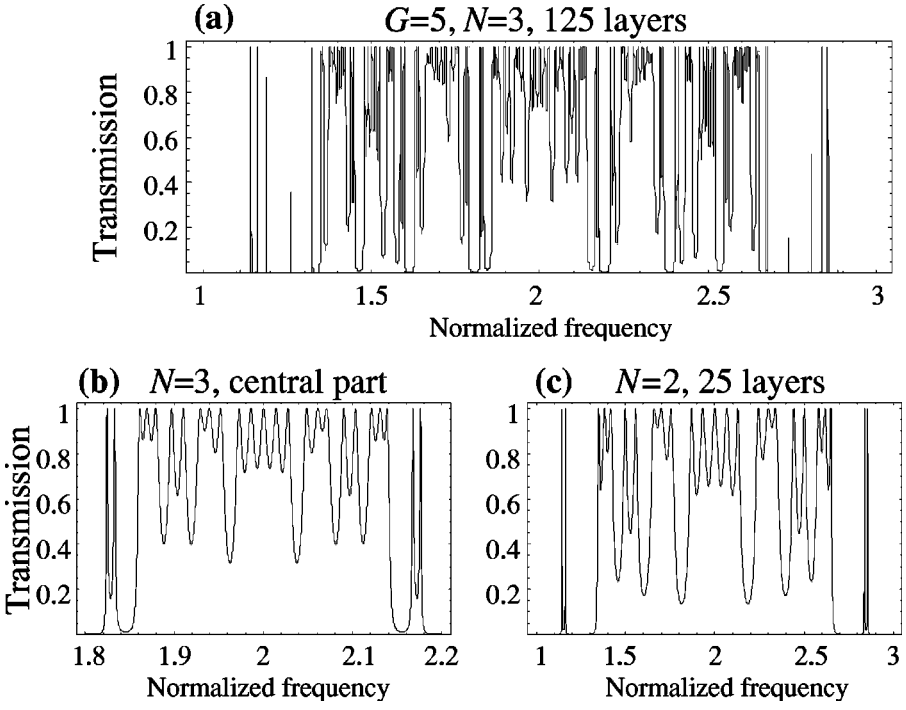

FIG. 5. Scalability of optical spectra for Cantor multilayers ($G=5$): the full period of a (3,4) spectrum (a) and the central part of it magnified in the frequency scale by 5 (b) versus the full period of a (3,3) spectrum (c). Comparing the looks of (b) and (c), one can see that the spectra are scalable with the factor equal to G.

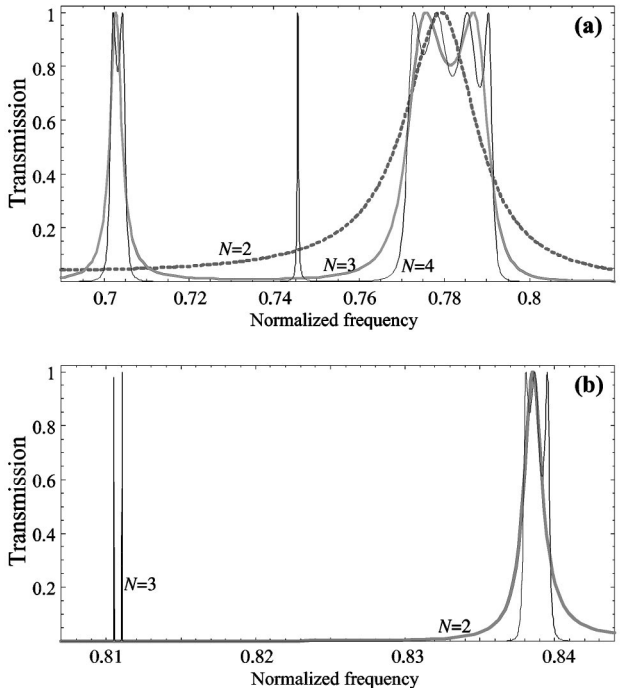

FIG. 6. Sequential splitting for $G=3$ (a) and $G=5$ (b). Note that the number of components in each multiplet is equal to that given by Eqs. (10) and (11). Also note that the half width of a resonance is almost the same before and after splitting.

$$S_{split}=\frac{G+1}{2} \tag{10}$$

and

$$S_{new}=\frac{G-1}{2}. \tag{11}$$

These relations state another connection between the geometrical and spectral properties of Cantor multilayers. Besides, note the half width of a peak is almost unchanged during splitting, while the external ''slopes'' of the whole multiplet become steeper [see Fig. 6(a)], and its envelope can be roughly characterized as ''rectangular.'' This effect can be made use of in optical band pass filters.

As an additional confirmation of the above-mentioned correlation, we have plotted the field intensity profiles ($|\mathbf{E}_\tau|^2$, to be exact, since it is this field component that undergoes no jumps at layer interfaces [28]) for the frequencies that correspond to the resonance peaks (components of both split multiplets and new ones). The field intensity for a multiplet is shown to be actually localized in the regions (cavities) that have been claimed responsible for the resonance peak at the relevant frequency (see Fig. 7). Thus, for the newly appeared multiplets the energy is strongly localized in newly appearing layers (binding areas). In split multiplets there is a pronounced localization in the previous generation substructures. As regards the difference between the field profiles for

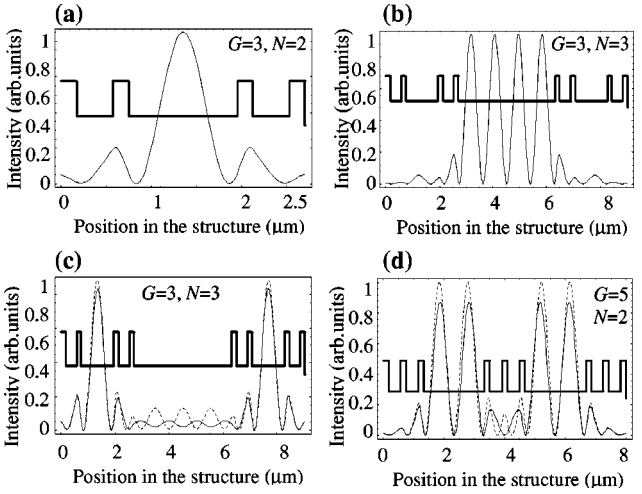

FIG. 7. Field intensity profiles for a newly appeared single peak in a (3,2) (a) and (3,3) (b), for a split doublet in a (3,3) (c), and for a newly appeared doublet in a (5,2) (d). z is the position inside the structure in the direction normal to the layer interfaces.

the individual multiplet components, it is only observed *outside* (and between) localization areas. This indicates that, for instance, in split multiplets the substructures are responsible for the peak itself while the binding causes it to split. Note that this splitting property is essentially the same as energy level splitting in adjacent quantum wells and bound pendulums in mechanics, and resonance splitting in connected electrical LC circuits in electricity.

Moreover, a closer look at the *resonance map* of the structure, i.e., a distribution of resonance peaks along the spectrum in dependence on the generation number (see Fig. 8), lets one see those points appear at determined places and constitute a definite pattern. This pattern apparently has scalability. If it possesses self-similarity as well, it would mean that the spectrum of transmission bands represents a fractal set. This property is already obtained for quasiperiodic multilayers, e.g., a resonance map for Fibonacci stacks is known to form a Cantor set [10]. It may well turn out to be that such behavior distinguishes this kind of media from both periodic and random ones, where no fractality at all is observed.

V. EXPERIMENT

Substitutional multilayer stacks of various types (Fibonacci, Thue-Morse, etc.) have been experimentally investigated (see, e.g., Ref. [19] and references therein). However, to the best of our knowledge, only analytical and numerical studies have been performed for model fractal structures. Here, we provide the experimental results for Cantor structures with smaller values of G and N.

We fabricated a lattice consisting of Na_3AlF_6 ($n_1=1.34$) and ZnS ($n_2=2.3$) using layer by layer vacuum deposition on a glass substrate, which is a standard optical technology. The optical thickness of every layer was made to equal 600 nm/4, i.e., $4d_1n_1=4d_2n_2=600$ nm, where d_1 and d_2 are geometrical thicknesses of the layers. Transmission spectra were measured using a ''Cary 500'' spectrophotometer.

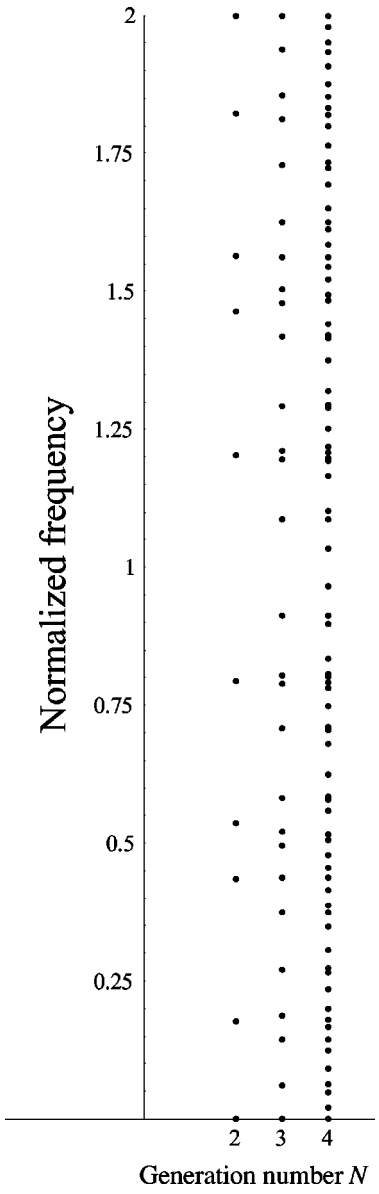

FIG. 8. Resonance map (frequencies of resonance peaks versus generation number) for a Cantor structure with $G=3$. One can see that new dots appear in a definite location, but seem to cover the whole frequency range. Thus, the problem of self-similarity of the transmission band spectra for Cantor structures requires further investigations.

As can be seen from Fig. 9, a good agreement with theoretically predicted spectrum is obtained. A formation of above-mentioned resonance transmission peaks is clearly seen, although all the effects are less pronounced due to the smaller contrast in refraction indices compared to that used for calculations for Fig. 4. This is the case because in numerical calculations the choice of the refraction indices for the media is not confined only to the ones suitable for experimental lattice fabrication.

The deviation of experimental spectrum [Fig. 9(a,b)] from the calculated one [Fig. 9(c,d)], which mainly occurs at the edges of the spectral interval examined, is caused by (i) absorption and dispersion effects of the materials used, (ii)

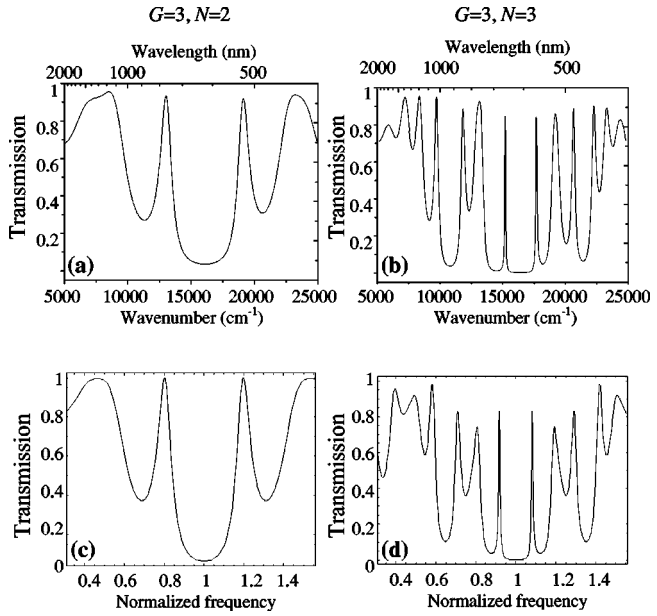

FIG. 9. Experimentally measured (a), (b) and calculated (c), (d) transmission spectra for Cantor structures with $G=3$, $N=2$ (a), (c) and $N=3$ (b), (d). The materials used were Na_3AlF_6 ($n_1=1.34$) and ZnS ($n_2=2.3$).

small fluctuations in layer thicknesses inevitable during vacuum deposition, and (iii) influence of the substrate. Thus, we have shown that the above-mentioned effects take place in real media, having at the same time checked the calculation procedure presented.

VI. SUMMARY AND CONCLUSIONS

To summarize, a wide variety of Cantor multilayer structures is systematically analyzed with respect to a resonant wave propagation. A simple and efficient numerical technique, which allows to calculate transmission and reflection spectra, as well as field intensity at any point inside the stack, is proposed. Using this technique, we found that transmission spectra possess two distinctive properties, *scalability* and *sequential splitting*. Both properties result from self-similarity of Cantor multilayers, and illustrate a clear and direct correlation between the geometry of a structure and the spectra of resonant transmission. The spatial field distribution patterns fully confirm the splitting mechanism, and aside from theoretical interest, these revealed properties can be useful for certain practical application, e.g., narrow band pass and band reject filters. The experimental studies naturally complete the work done on Cantor multilayers, confirming the numerical results obtained.

The established connection between geometrical and spectral properties leads to another consideration. There are structures shown to have fractal self-similar transmission spectra (Fibonacci lattices at least, see Ref. [10]), and Cantor structures are geometrically fractal. Putting these facts together, this may mean that spectra of Cantor structures are fractal as well. However, self-similarity in not clearly pro-

nounced in Cantor spectra, as is the case with Fibonacci, and the peak locations on the resonance map (see Fig. 8) do not at all remind of Cantor dust. Evidently, this problem requires further investigations, and we expect that answers will be found in the forthcoming papers.

ACKNOWLEDGMENTS

Helpful discussions with D. N. Chigrin are acknowledged. This work was supported in part by the Basic Research Foundation of Belarus.

[1] J. D. Joannopoulos, R. D. Meade, and J. N. Winn, *Photonic Crystals: Molding the Flow of Light* (Princeton University Press, Princeton, 1995).
[2] J. T. Londergan, J. P. Carini, and D. P. Murdock, *Binding and Scattering in Two-Dimensional Systems: Application to Quantum Wires, Waveguides, and Photonic Crystals* (Springer-Verlag, New York, 1999).
[3] D. N. Chigrin, A. V. Lavrinenko, D. A. Yarolsky, and S. V. Gaponenko, IEEE J. Lightwave Tech. **17**, 2018 (1999).
[4] S. John, Phys. Rev. Lett. **53**, 2169 (1984).
[5] P. Anderson, Philos. Mag. B **52**, 505 (1985).
[6] D. S. Wiersma, P. Bartolini, A. Lagendijk, and R. Righini, Nature (London) **390**, 671 (1997).
[7] Y. Gefen, B. B. Mandelbrot, and A. Aharony, Phys. Rev. Lett. **45**, 855 (1980).
[8] Y. Gefen, A. Aharony, B. B. Mandelbrot, and S. Kirkpatrick, Phys. Rev. Lett. **47**, 1771 (1981).
[9] R. B. Griffiths and M. Kaufman, Phys. Rev. B **26**, 5022 (1982).
[10] M. Kohmoto and B. Sutherland, Phys. Rev. B **35**, 1020 (1987).
[11] Y. Z. Peng and T. Y. Fan, J. Phys.: Condens. Matter **12**, 9381 (2000).
[12] E. Macia, Phys. Rev. B **61**, 6645 (2000).
[13] E. Macia, Phys. Rev. B **60**, 10 032 (1999).
[14] E. Macia, Appl. Phys. Lett. **73**, 3330 (1998).
[15] X. Huang, Y. Wang, and C. Gong, J. Phys.: Condens. Matter **11**, 7645 (1999).
[16] R. W. Peng, M. Wang, A. Hu, S. S. Jiang, G. J. Jin, and D. Feng, Phys. Rev. B **57**, 1544 (1998).
[17] D. H. A. L. Anselmo, M. G. Cottam, and E. L. Albuquerque, J. Phys.: Condens. Matter **12**, 1041 (2000).
[18] C. G. Berzera, E. L. Albuquerque, and E. Nogueira, Jr., Physica A **267**, 124 (1999).
[19] M. S. Vasconcelos and E. L. Albuquerque, Phys. Rev. B **57**, 2826 (1998).
[20] A. Ghosh and S. N. Karmakar, Phys. Rev. B **57**, 2834 (1998).
[21] C. Allain and M. Cloitre, Phys. Rev. B **33**, 3566 (1986).
[22] C. Sibilia, I. S. Nefedov, M. Scalora, and M. Bertolotti, J. Opt. Soc. Am. B **15**, 1947 (1998).
[23] C. Sibilia and M. Bertolotti, in ICO Book IV *Trends in Optics and Photonics*, edited by T. Asakura (Springer-Verlag, New York, 1999), and references therein.
[24] H. Hattori, V. Schneider, and O. Lisboa, J. Opt. Soc. Am. A **17**, 1583 (2000).
[25] A. Chakrabarti, Phys. Rev. B **60**, 10 576 (1999).
[26] J. Feder, *Fractals* (Plenum Press, New York, 1988).
[27] L. Brekhovskikh, *Waves in Layered Media* (Nauka, Moscow, 1960).
[28] M. Born and E. Wolf, *Principles of Optics* (Cambridge University Press, Cambridge, 1999).
[29] A. Yariv and P. Yeh, *Optical Waves in Crystals* (Wiley, New York, 1984).
[30] P. Yeh, *Optical Waves in Layered Media* (Wiley, New York, 1988).
[31] S. Solimeno, B. Crosignani, and P. Di Porto, *Guiding, Diffraction, and Confinement of Optical Radiation* (Academic Press, Orlando, 1986).